

# Experimental Characterization of Aerosol Suspension in a Rotating Drum

Sheng-Hsiu Huang<sup>1</sup>, Yu-Mei Kuo<sup>2\*</sup>, Chih-Wei Lin<sup>1</sup>, Wei-Ren Ke<sup>1</sup>, Chih-Chieh Chen<sup>1\*\*</sup>

<sup>1</sup>*Institute of Occupational Medicine and Industrial Hygiene, College of Public Health, National Taiwan University, Rm. 718, No. 17, Xu-Zhou Rd., Taipei 100, Taiwan*

<sup>2</sup>*Department of Occupational Safety and Health, Chung Hwa University of Medical Technology, No. 89, Wen-Hwa 1st Street, Jen-Te District, Tainan 717, Taiwan*

## Abstract

Rotating drum chambers are simple and effective devices for retaining particles in airborne state for prolonged periods. Many studies including inhalation toxicology, environmental fate, and survivability of airborne pathogens could benefit from using them. Particle size is the major factor governing aerosol suspension. Yet reliable experimental data as a function of particle size on the optimal rotation rate are limited. Therefore, this study aims to experimentally characterize a rotating drum and to optimize the operation rate for the bioaerosol size spectrum. Moreover, the sampling methodology for evaluating the performance of a rotating drum is also investigated. Charge-neutralized potassium sodium tartrate (PST) particles generated by an ultrasonic atomizer are used as surrogates of bioaerosols to characterize the performance of the rotating drum. Aerosol number concentrations and size distributions in the rotating drum are continuously or intermittently measured by an aerodynamic particle sizer (APS) in real time. Then the decay constants of aerosol number concentrations as a function of particle size, elapsed time, and rotation rate are calculated, respectively. Experimental results revealed that the rotation of a drum chamber enhances particle suspension greatly and the rotating rate can be optimized to retain the suspended particles for an extended time period. With the current drum geometry, the optimal rotation rate varies from 2 to 7 rpm in the particle size range of 1 to 7  $\mu\text{m}$  and is proportional to particle size. When operating at the optimal rotation rate (2-4 rpm), 5% of 1- $\mu\text{m}$  particles can remain suspended for over 24 hours. However, it is crucial to adjust the optimal rate carefully for large particles and long suspension duration.

**Keywords:** Rotating drum, Decay constant, Suspension time, Optimal rotating rate

---

\*Corresponding author. Tel: 886-912017249; Fax: 886-6-2894028

E-mail address: [ymkuo@mail.hwai.edu.tw](mailto:ymkuo@mail.hwai.edu.tw)

\*\* Corresponding author. Tel: 886-928253663; Fax: 886-2-23938631

E-mail address: [ccchen@ntu.edu.tw](mailto:ccchen@ntu.edu.tw)

35

## 36 INTRODUCTION

37 Many infectious organisms including viruses, bacteria, and fungi have been shown to be  
38 transmitted by the airborne route. The ability of these microorganisms to survive in airborne state  
39 plays a key role in their aerial dissemination. Therefore, besides recommending good personal  
40 hygiene practices, many researchers tried to formulate environmental control guidelines through  
41 investigating the effects of factors such as temperature, relative humidity, and light or chemicals  
42 exposure on promoting or retarding the survival of infectious organisms in the air. However,  
43 results on airborne survival of microorganisms from previous studies varied considerably due to  
44 different experimental techniques used. Thus, a well-characterized experimental system is  
45 essential for making generalized conclusions and developing mathematical models.

46 Many measures have been developed to control the infectiveness of airborne pathogens  
47 (Huang et al., 2012; Chen et al., 2016). The key to validate the effectiveness of control measures  
48 is to retain the microorganisms in aerosol phase for prolonged periods of time. However, the  
49 suspension of bioaerosols is subjected to gravitational settling in a stationary test chamber.  
50 Although keeping the aerosols in stationary chambers with gently stirring would delay  
51 sedimentation, large particles still need long settling distances to extend the airborne period.  
52 Alternatively, a rotating drum (Goldberg et al., 1958), which is an uncomplicated but more  
53 effective device, was shown to be capable of retaining particles in airborne state for prolonged  
54 periods. Experimentally, as compared with a stirred settling aerosol chamber 1 m in height,  
55 almost a 20-fold increase in duration of holding time for 1- $\mu\text{m}$  particles in a 1-m-diameter drum  
56 chamber rotated at 2 rpm is demonstrated (Goldberg, 1971). Another subsequent study generated  
57 Di-n-hexyl phthalate (DHP) particles with a 0.8- $\mu\text{m}$  mass median diameter in a 40-cm-diameter  
58 drum and found a 90% reduction of the particle settling loss as the drum rotated at about 3 rpm  
59 (Frostling, 1973). However, bacterial and fungal aerosols in indoor environment are usually in the

60 size range of 3  $\mu\text{m}$  in count median diameter (CMD) which is much larger than those tested in the  
61 previous studies (Kuo, 2015). Even though the aerosol decay as a function of particle size in a  
62 rotating drum chamber has been comprehensively studied using advanced particle sizing  
63 instruments (Embury and Sutton, 2005; Sutton, 2005), several issues that can affect the results  
64 have not been addressed. Since aerosol charge neutralizers were not used, their data would reflect  
65 the influence of particle charge. Furthermore, the high particle number concentrations used in  
66 these studies might cause significant coincidence errors in the APS counts.

67 In rotating drum chambers, particles remain suspended as a result of the competition  
68 between gravitational and centrifugal forces. At high drum rotation rate, the centrifugal force is  
69 the dominant aerosol deposition mechanism. Taking into account the combined effects of  
70 gravitational and centrifugal forces, Gruel et al. (1987) developed an equation to predict the  
71 fraction of suspended particles by assuming that the aerosols in the rotating chamber decay  
72 exponentially (referred to as Gruel's model). The fraction of suspended particles is

$$73 \quad \frac{N}{N_0} = \left[ \frac{(R-r_0)^2}{R^2} \right] \exp(-2\tau\omega^2 t) \quad (1)$$

74 where  $N$  and  $N_0$  are number of particles and initial number of particles in drum, respectively;  $R$  is  
75 the drum radius;  $r_0$  is the radius of gyration of a particle in the rotating drum ( $r_0 = \tau g/\omega$ );  $\tau$ ,  $g$   
76 and  $\omega$  are the particle relaxation time, gravitational acceleration and angular velocity of drum  
77 rotation, respectively; and  $t$  is the time beginning after one revolution.

78 Gruel's model is appropriate for predicting the fraction of suspended particles after one  
79 revolution when centrifugal force is much less than gravitational force (Embury and Sutton,  
80 2005). However, it is not applicable when the rotation rate is reduced to zero because the solution  
81 does not converge to the gravitational settling solution (Asgharian and Moss, 1992). Therefore,  
82 Asgharian and Moss (1992) used the concept of limiting trajectories of the suspended particles

83 that proposed by Pich (1972) to predict the fraction of suspended particles as a result of the  
 84 combined effects of gravity and centrifugation over the complete range of rotation rates (referred  
 85 to as Moss's model). The fraction of suspended particles is

$$86 \quad \frac{N}{N_0} = 1 - \frac{1}{\pi} \left[ \frac{y_p}{R} \sqrt{1 - \left( \frac{y_p}{2R} \right)^2} + 2 \sin^{-1} \frac{y_p}{2R} \right] \quad \text{for } 0 \text{ rpm} \quad (2)$$

$$87 \quad \frac{N}{N_0} = \exp(-2\tau\omega^2 t) \quad \text{for } \frac{H}{R} \leq 1 - \exp(-\tau\omega^2 t) \quad (3)$$

$$88 \quad \frac{N}{N_0} = \frac{1 + \exp(-2\tau\omega^2 t)}{2} - \frac{1}{\pi} \left[ \frac{H_1}{R} \sqrt{1 - \left( \frac{H_1}{R} \right)^2} + \sin^{-1} \frac{H_1}{R} + \frac{H_2}{R} \sqrt{\exp(-2\tau\omega^2 t) - \left( \frac{H_2}{R} \right)^2} + \right. \\ \left. \exp(-2\tau\omega^2 t) \sin^{-1} \left( \frac{H_2}{R} \right) \right] \\ 89 \quad \text{for } 1 - \exp(-\tau\omega^2 t) \leq \frac{H}{R} \leq 1 + \exp(-\tau\omega^2 t) \quad (4)$$

$$90 \quad \frac{N}{N_0} = 0 \quad \text{for } \frac{H}{R} \geq 1 + \exp(-\tau\omega^2 t) \quad (5)$$

91 where

$$92 \quad y_p = \tau g t - \tau^2 g (1 - \exp^{-t/\tau})$$

$$93 \quad H = \frac{\tau g}{\omega} \sqrt{1 - 2 \cos(\omega t) \exp(-\tau\omega^2 t) + \exp(-2\tau\omega^2 t)} \quad \text{for } \omega t < \pi$$

$$94 \quad H = \frac{\tau g}{\omega} [1 + \exp(-\tau\omega^2 t)] \quad \text{for } \omega t > \pi$$

$$95 \quad H_1 = \frac{R^2 + H^2 - R^2 \exp(-2\tau\omega^2 t)}{2H}$$

$$96 \quad H_2 = H - H_1$$

97 and t here is the time begins as the first revolution begins. It should be noted that the parameter  
 98 "time" in Moss's equation is different from that defined in Gruel's equation (or Eq. (1)).

99 The rotating drum has been extensively employed to study the retention of microorganisms  
100 in aerosol phase and the decay of bioaerosols under a variety of environmental conditions, such  
101 as relative humidity, temperature, UV, ozone, germicides, gaseous pollutants and so forth.  
102 (Krumins et al., 2008; Verreault et al., 2008; Piercy et al., 2010; Santarpia et al., 2012; Verreault  
103 et al., 2013; Santarpia et al., 2014; Verreault et al., 2014; Ratnesar-Shumate et al., 2015; Johnson  
104 et al., 2016; Turgeon et al., 2016; Haddrell and Thomas, 2017). However, the bioaerosol decay  
105 measured in these studies is a combination of biological decay and physical decay. It is important  
106 to evaluate the physical decay of aerosols in a rotating drum so as to elucidate the actual  
107 effectiveness of the studied parameters. Moreover, the deposition of aerosols is a function of  
108 particle size and it is crucial to characterize the physical decay for the bioaerosol size spectrum in  
109 a rotating chamber to optimize the rotation rate for prolonged aerosol suspension time period.

110 An endeavor has been made to experimentally investigate the aerosol physical decay as a  
111 function of particle size, suspension time and rotation rate in a rotating chamber by Sutton and  
112 colleague (Embury and Sutton, 2005; Sutton, 2005). The aerosol decay experiments are  
113 conducted in a 1-m-diameter drum chamber with a piston inside the drum to pull air into or out of  
114 the drum which is different from Goldberg's rotating drum. However, some of the experimental  
115 results reveal a need for further improvements. First, the test particles failed to show a bimodal  
116 distribution with peaks at 3 and 6  $\mu\text{m}$  as expected due to triboelectric charging. The test particles  
117 were generated pneumatically in a large plastic bag using a sonic nozzle. The size distribution  
118 and concentration of challenged aerosols are not well controlled to minimize the measurement  
119 bias. Moreover, some experimental data are not reasonable. For example, the aerosol decay  
120 results of 3 rpm test did not fall in line with those of 2 and 4 rpm tests and the concentrations of  
121 1- and 2- $\mu\text{m}$  particles increased within the first 4 to 6 hours for some of the tests. These

122 discrepancies have not been addressed. Finally, Sutton's experimental measurements and Moss's  
123 model agreed only qualitatively but not quantitatively.

124 In this study, some improvements have been made to obtain reliable measurement data. The  
125 test aerosols were generated and neutralized before introduced into the drum chamber to  
126 eliminate the measurement bias due to triboelectric charging. Furthermore, the initial aerosol  
127 concentration in the rotating drum was well controlled at a low concentration (approximately 170  
128 particles/cm<sup>3</sup>) to reduce aerosol coagulation. The size distribution of the test aerosols meets the  
129 designate size range of different types of bioaerosols. To make the best use of rotating drum  
130 chambers in bioaerosol aging studies, this study aims to characterize the aerosol decay in a  
131 rotating drum, to determine the optimal rotation rate as a function of particle size, and to compare  
132 the theoretical predictions of Gruel's and Moss's models with experimental measurements.

## 133 **METHODS**

134 The experimental system comprises two compartments, the aerosol generation system and  
135 the rotatable drum unit as illustrated in Fig. 1. An ultrasonic atomizer (Model 8700-120MS,  
136 Sono-Tek Corporation, Poughkeepsie, NY, USA) is adopted to generate micrometer-sized PST  
137 (potassium sodium tartrate tetrahydrate, density 1.79 g/cm<sup>3</sup>, KOCO(CHOH)<sub>2</sub>COONa· 4H<sub>2</sub>O,  
138 A.C.S. grade, J.T.Baker®, Center Valley, PA, USA) particles as surrogates of bioaerosols. A  
139 syringe pump (KDS 200 / 200P, KD Scientific Inc., Holliston, MA, USA) is employed to deliver  
140 the solution to the ultrasonic atomizer to generate test particles. Then the particles are neutralized  
141 to the Boltzmann charge equilibrium using an aerosol neutralizer (10-mCi Am-241 radioactive  
142 source). The aerosol output is diluted with filtered, dried compressed air in an aerosol capacitance  
143 chamber which is 20 cm in diameter and 100 cm in height. Previous research (Ho, 2006) showed  
144 that the aerosol decay can be biased by aerosol coagulation when the initial aerosol concentration  
145 exceeds 10<sup>5</sup> particles/cm<sup>3</sup>. To avoid measurement bias due to aerosol coagulation, the dilution air

146 is set at a flow rate of 60 L/min. An aerodynamic particle sizer (APS, Model 3321, TSI Inc., St.  
147 Paul, MN, USA) is employed to measure the aerosol number concentration and distribution in the  
148 aerodynamic size range of 0.5-20  $\mu\text{m}$ . The APS can measure particle number concentration up to  
149 1000 counts/cm<sup>3</sup> at diameters of 0.5 and 10  $\mu\text{m}$  with coincidence errors less than 5% and 10%,  
150 respectively (TSI, 2012).

151 The acrylic rotating drum is 0.29 m in inner diameter and 0.59 m in length with a total  
152 volume of 39 L. The drum is mounted on a rack to allow free rotation on a horizontal axis and  
153 connected to an electric motor with a belt to attain the required rotation rate. Probes and sampling  
154 ports are installed on the non-rotating part of the drum. The temperature and relative humidity  
155 inside the chamber are monitored with a Temp/RH probe (HP 22, Rotronic Inc., Switzerland). A  
156 stainless tube, 0.34 m long by 4.2 mm inner diameter, is inserted into the drum with the inlet of  
157 the sampling probe positioned in the center of the rotating chamber. The outlet of the sampling  
158 probe is directly connected to the inner nozzle of the APS. Before each experiment, the chamber  
159 is purged with filtered compressed air until no aerosols are detected by the APS. The test aerosols  
160 are introduced into the rotating drum through the “A” valve and the excess air is vented through  
161 the “B” valve as illustrated in Fig. 1. Aerosols are introduced into the drum chamber for about 6  
162 minutes to reach a stable particle concentration of approximately 170 particles/cm<sup>3</sup> during the  
163 drum experiments to prevent measurement bias due to coagulation effect. Then both “A” and “B”  
164 valves are closed and the air duct connecting the aerosol capacitance chamber and the rotating  
165 chamber is disconnected. The drum operates at the assigned rotating rate and the APS samples at  
166 1 L/min. To balance for air loss to sampling, 2 L/min filtered compressed air is supplied into the  
167 drum through “C” valve and the excess air was vented. All the measurements are conducted in  
168 triplicate unless otherwise stated.

169 To examine the aerosol decay over time, the mean aerosol concentration after certain  
170 suspension period is divided by the initial aerosol concentration to obtain the suspended aerosol  
171 fraction. Goldberg (1958) assumed that the aerosol decay in a rotating drum could be expressed  
172 as a constant percent loss per unit time by the following equation.

$$173 \quad N = N_0 \exp^{-kt} \quad (6)$$

174 where  $N_0$  is the initial aerosol number or concentration,  $N$  is the aerosol number or concentration  
175 after time  $t$ , and  $k$  is the aerosol decay constant. This first-order model for aerosol decay is  
176 governed by the particle aerodynamic properties and rotation rate of the drum.

## 177 **RESULTS AND DISCUSSION**

### 178 *Bias versus sampling protocols*

179 To evaluate the bias from dilution effect due to sampling, an experimental system is built as  
180 illustrated in the upper left box of Fig. 1. Ambient aerosols with a count median diameter (CMD)  
181 of 102 nm and a geometric standard deviation (GSD) of 1.98 are introduced into the rotating  
182 chamber to alleviate the effects of gravitational settling and centrifugal impaction. The total  
183 aerosol concentration is continuously monitored by a condensable particle counter (CPC, model  
184 3022A, TSI Inc., St. Paul, MN, USA) at an inlet flow rate of 1 L/min under the drum rotation  
185 rates of 0, 5 and 20 rpm, respectively. Figure 2 shows the suspended aerosol fraction as a function  
186 of time during continuous sampling. No significant difference is found for the aerosol decay  
187 under different rotation rates. This is because the influence of gravity and rotation are both  
188 negligible for the sub-micrometer-sized aerosols being tested. As for aerosol dilution caused by  
189 sampling, the resulting decay constant is estimated to be  $0.033 \text{ min}^{-1}$ . It can be inferred that the  
190 total sampling time for completing the experiment is not allowed to exceed 93 seconds assuming  
191 a 5% tolerance of error. Otherwise, the dilution effect should be adjusted to obtain true decay  
192 constants.



193 According to the experimental setup shown in Fig. 1, it takes only 39 minutes to replace the  
194 air volume of the drum chamber under an ideal plug flow condition. Two sampling approaches  
195 including continuous sampling and intermittent sampling on the aerosol decay measurement are  
196 compared. The test aerosols with a CMD of 5.16  $\mu\text{m}$  and a GSD of 1.67 are generated and  
197 introduced into the rotating chamber. Owing to the small radius of the drum used in this work, the  
198 drum is operated at a rotation rate of 5 rpm to retain more particles suspended than in a stationary  
199 drum chamber. For continuous sampling, the aerosol concentration in the rotating chamber is  
200 continuously monitored by the APS at 1 L/min throughout the 1-hr suspension period. As for  
201 intermittent sampling, the APS samples for 1 minute only at the beginning and at the end of the  
202 1-hr suspension period with no air sampling in between. Approximately 5% air is withdrawn  
203 from the rotating chamber and the resulting bias on the aerosol decay measurement should be  
204 negligible. Figure 3 compares the suspended aerosol fraction versus particle size for both  
205 continuous and intermittent sampling after 1-hr suspension period. As is expected, larger particles  
206 decay faster than small particles due to gravitational settling. Moreover, the aerosol decay in the  
207 rotating chamber is significantly biased by continuous sampling and the calculated aerosol decay  
208 rates under continuous sampling are seven times more than those under intermittent sampling,  
209 especially for particles smaller than 5  $\mu\text{m}$ . To avoid the bias from sampling protocol, the  
210 intermittent sampling approach with total sampling time not exceeding the abovementioned  
211 limitation (93 seconds) is adopted for the remaining experiments, unless otherwise specified.

### 212 *Aerosol decay versus particle size*

213 The aerosol concentrations in the rotating drum with a rotation rate of 5 rpm are measured  
214 by the APS for a sampling period of 15 seconds in every 15 minutes throughout the 1-hr  
215 suspension period. Figure 4 shows the aerosol decay over time for particle sizes of 1, 3, 5.1 and  
216 7.2  $\mu\text{m}$ . The straight lines demonstrate that the aerosol concentrations for each particle size in the

217 rotating chamber follow a first-order exponential decay. Moreover, larger particles decay faster  
218 than smaller particles as expected. The calculated decay constants for 1-, 3-, 5.1- and 7.2- $\mu\text{m}$   
219 particles are  $0.0033 \pm 0.0006$ ,  $0.0084 \pm 0.0003$ ,  $0.016 \pm 0.002$ , and  $0.059 \pm 0.005 \text{ min}^{-1}$ ,  
220 respectively. These results imply that the aerosol decay kinetics inside the rotating drum for  
221 different particle sizes can be estimated using the extrapolation method according to the decay  
222 constant calculated using short-term measurements of aerosol decay kinetics.

### 223 *Aerosol decay as a function of time*

224 To evaluate the aerosol decay over time inside a rotating drum, the test aerosols with a  
225 CMD of  $5.16 \mu\text{m}$  and a GSD of 1.67 are generated and introduced into the drum which rotated at  
226 5 rpm. The aerosol number concentrations as function of aerosol size, after rotating for 1, 4 and  
227 24 hours are measured by the APS. Figure 5 shows the fraction of initial particles that remain  
228 suspended as functions of particle size and suspension time. The aerosols in the rotating chamber  
229 decay dramatically with increasing suspension time. For 1- $\mu\text{m}$  particles, the suspended aerosol  
230 fractions are 92, 73 and 14% after 1, 4 and 24 hours of suspension, respectively. Moreover,  
231 aerosol decay tendency is more prominent for the beginning of the test as the particle size  
232 increases. For example, the suspended aerosol fraction for 2- $\mu\text{m}$  particles varies from 80% for  
233 1-hr suspension to 48% after 4-hr suspension as compared with the corresponding levels for  
234 1- $\mu\text{m}$  particles. The solid lines represent the results calculated using the extrapolation method  
235 according to the decay constants obtained from the aerosol decay kinetic measurements of  
236 half-hour suspension period. As can be observed, the calculated results match well with the  
237 measurements of 1, 4, and 24-hr suspension period. It is proved again that the aerosol  
238 concentration over an extended period of suspension time in a rotating chamber can be predicted  
239 using the decay constant measured within a limited time period.

240 Evidence shows that the retention of aerosols in rotating drums is less efficient than the  
241 theoretical predicted data (Frostling, 1973; Sutton, 2005; Verreault et al., 2013; Verreault et al.,  
242 2014). To comprehensively compare the experimental measurements with the existing  
243 mathematical models, the fractions of suspended aerosols in the rotating drum as a function of  
244 particle size are calculated for the suspension durations of 1, 4 and 24 hours using Eqs. (1) and  
245 (3). Results of the calculations are also shown in Fig. 5 with the long-dash and dotted lines  
246 representing the predictions of Gruel's model and Moss's model, respectively. Figure 6 shows the  
247 ratio of experimental measurements and theoretical solutions using the two models. Both  
248 mathematical models are found to significantly underestimate the aerosol decay in the rotating  
249 drum. For 1-hr suspension time period, both Gruel's and Moss's models predict correctly the  
250 suspended aerosol fraction for particles smaller than 5  $\mu\text{m}$ . For those particles larger than 5  $\mu\text{m}$ ,  
251 the differences between experimental and theoretical data may be partly attributed to  
252 measurement bias because there are fewer particles of larger size after suspension duration. In  
253 addition, as the challenged particles were injected into the drum chamber through the "A" valve,  
254 this will affect the flow pattern inside the drum and the entering particles with some velocity  
255 diffuse throughout the chamber volume will inevitably affect their path. The aerosol  
256 concentration inside the chamber is initially not uniform. Eventually, the particles will become  
257 fairly uniform throughout the chamber volume as stirred settling model is appropriate for  
258 turbulent mixing due to the incoming particle flow and convective mixing due to small  
259 temperature differences between air and chamber wall (Fuchs, 1964). On the other hand, it should  
260 be noted that only gravitational and viscous drag forces are relevant and taken into consideration  
261 in the mathematical models of Gruel and Moss (Gruel et al., 1987; Asgharian and Moss, 1992).  
262 The aerosol motion along the horizontal axis is ignored. Forces due to electrostatic, diffusion,  
263 pressure gradient and mutual collision are also not considered. In addition, as the drum is

264 assumed to be maintained in an isothermal condition, thermal gradient forces are excluded in the  
265 models. In a real situation, the gravitational gyration becomes the dominant transport mechanism  
266 as the drum starts to rotate. Sutton claimed that electrostatic forces due to triboelectric charging  
267 play an important role in determining the aerosol decay (Sutton, 2005). However, significant  
268 differences between our experimental data and Moss's mathematical model are still found after  
269 the effect of electrostatic forces was excluded by aerosol neutralization in this work. Convective  
270 diffusion is another possible mechanism proposed by Sutton (2005). However, no satisfactory  
271 explanation can be made due to the limitation of this experiment.

### 272 *Aerosol decay as a function of rotation rate*

273 The fractions of suspended particles are measured at the rotation rate varying from 0 to 20  
274 rpm for 1-hr suspension time period. For better clarity, only the results of 0, 5 and 20 rpm are  
275 plotted in Fig. 7. As can be seen, the rotating drum chamber yields more suspended particles at 5  
276 rpm than at stationary phase (0 rpm) and 20 rpm. For 2- $\mu\text{m}$  particles, the fraction of suspended  
277 particles is 84% for 5 rpm but only 14 and 45% for the drum rotated at 0 and 20 rpm, respectively.  
278 The experimental results imply that the rotation of a drum chamber greatly enhances particle  
279 suspension and the rotating rate can be optimized to retain the suspended particles for an  
280 extended time period.

281 The theoretical model predictions of Gruel and Moss for different rotation rates are also  
282 shown in Fig. 7 as long-dashed and dotted lines, respectively. For the current drum geometry  
283 (drum radius = 14.5 cm), particles larger than 1.5  $\mu\text{m}$  will deposit at the wall of a stationary drum  
284 (0 rpm) for 1-hr measurement time as estimated by Eq. (2) (also referred to as Moss's model).  
285 The mathematical model underestimated the fraction of suspended particles in a stationary drum.  
286 The underestimation may be due to convective or turbulent mixing caused by air compensation  
287 for sampling loss. When the drum starts to rotate, both models predict identical results on the

288 fraction of suspended particles at high rotation rate (20 rpm) and yield slight differences at low  
289 rotation rate (5 rpm) indicating the combined effect of gravitational settling and centrifugal  
290 deposition. In general, mathematical models tend to overestimate the fraction of suspended  
291 particles when the drum chamber is rotating and this is in good agreement with the findings of  
292 previous studies (Embury and Sutton, 2005; Sutton, 2005). Figure 8 shows the ratio of  
293 experimental measurements and numerical data at 0, 5 and 20 rpm, as a function of particle size.  
294 Both mathematical models predict accurately the suspended aerosol fraction for particles smaller  
295 than 5  $\mu\text{m}$  at 5 rpm. However, particle residence is dramatically overestimated especially for  
296 larger particles at higher rotation rate. As abovementioned, the real case is likely very  
297 complicated whereas only gravitational and viscous drag forces were taken into consideration in  
298 the existing models.

#### 299 ***Optimal rotation rate versus particle size***

300 The particle size and rotation rate-dependent aerosol decay constants are plotted in Fig. 9. It  
301 is evident that there is a minimal decay constant for each particle size in the measured rotation  
302 rate range, implying that the drum rotation rate can be optimized to retain suspended particles for  
303 an extended time period during the experiments when the gravity force and centrifugal force are  
304 comparable in magnitude. An interesting trend of increase in optimal rotation rate with increasing  
305 particle size is observed. The optimal rotation rate as a function of particle size is shown in Fig.  
306 10 and the optimal rotation rate ( $V$  in rpm) is found to be accurately predicted with particle size  
307 ( $d_p$  in  $\mu\text{m}$ ) by the following equation.

$$308 \quad V = 0.6007d_p + 1.9159 \quad (7)$$

309 The optimal rotation rate varies from 2 to 7 rpm in the particle size range of 1 to 7  $\mu\text{m}$  and is  
310 proportional to particle size. This finding is in agreement with Sutton's experimental results that  
311 the optimal rotation rate falls between 1 and 6 rpm (Sutton, 2005). As a rough estimate, it would

312 be a good guess to choose 5 rpm for prolonged residence time periods for the potential bioaerosol  
313 size spectrum in aging studies based on our experimental findings. However, such predicted  
314 result is inconsistent with the numerical studies of Gruel et al. (1987) and Asgharian and Moss  
315 (1992). The optimal rotation rate is concluded to be independent of particle size for particles  
316 smaller than 10  $\mu\text{m}$  (Gruel et al., 1987) or 5  $\mu\text{m}$  (Asgharian and Moss, 1992). Moreover, the  
317 optimum rotation rates predicted by Moss's model for all particle sizes are quite similar and vary  
318 from 0.29 to 1.41 rpm which is much lower than the experimental results obtained in this study  
319 and the previous study (Embury and Sutton, 2005).

320 For practical application of a rotating drum chamber in bioaerosol aging experiments, it is  
321 critical to retain the test microorganisms in aerosol phase throughout the experimental process.  
322 Figure 11 shows aerosol residence time isopleths. Aerosol residence time is defined as the time  
323 that 5% of initial suspended particles remain suspended and is calculated given the rotation rate  
324 and aerosol decay constant are known. With the current drum geometry used in this work, the  
325 optimal rotation rate between 2 and 4 rpm can suspend 1- $\mu\text{m}$  particles for over 24 hours. The  
326 operating range of drum rotation rate for large particles and long residence time is narrower than  
327 that for small particles and short residence time, implying greater care required when adjusting  
328 the optimal rate for large particles and long suspension duration.

## 329 **CONCLUSIONS AND RECOMMENDATIONS**

330 This study investigates the effects of various critical parameters on decay constants of  
331 aerosols in the drum chamber. Experimental results are also compared with theoretical  
332 predictions from two previous models of aerosol dynamics in a rotating drum. Since the  
333 continuous sampling approach results in underestimation of the aerosol decay constants due to  
334 the dilution effect, the following conclusions are drawn from the experimental results according  
335 to the intermittent sampling protocol.

336 For micrometer-sized particles, a considerable delay of sedimentation can be achieved using  
337 the rotating drum. It is demonstrated that the aerosol concentration over an extended period of  
338 suspension time in a rotating chamber can be predicted using the decay constant, measured within  
339 a limited time period. With the current drum geometry, the optimal rotation rate varies from 2 to  
340 7 rpm in the particle size range of 1 to 7  $\mu\text{m}$  and is linearly proportional to particle size. When  
341 operating at the optimal rotation rate (2~4 rpm), 5% of 1- $\mu\text{m}$  particles can remain suspended for  
342 over 24 hours. However, it is crucial to adjust the optimal rate carefully for large particles and  
343 long suspension duration. Although there are discrepancies between Moss's model and the  
344 experimental data and remain unresolved, the rotating drum chamber is still a useful tool and 5  
345 rpm is recommended for bioaerosol aging studies.

346

#### 347 **ACKNOWLEDGMENTS**

348

349 This research was financially supported by the Ministry of Science and Technology, Taiwan,  
350 R. O. C. under the grant: MOST 103-2221-E-273 -002 -MY2.

351

#### 352 **REFERENCES**

353

354 Asgharian, B. and Moss, O.R. (1992). Particle Suspension in a Rotating Drum Chamber When  
355 the Influence of Gravity and Rotation Are Both Significant. *Aerosol Sci. Technol.* 7:  
356 263-277.

357 Chen, J.W., Lee, W.M., Chen, K.J. and Yang, S.H. (2016). Control of Bioaerosols in Indoor  
358 Environment by Filter Coated with Nanosilicate Platelet Supported Silver Nanohybrid  
359 (AgNPs/NSP). *Aerosol Air Qual. Res.* 16: 2198-2207.

360 Embury, J.F. and Sutton, T.A. (2005). Analysis of Aerosol Aging in the Rotating Drum Chamber.  
361 S. Army research, development and engineering command.

362 Frostling, H. (1973). A Rotating Drum for the Study of Toxic Substances in Aerosol Form. *J.*  
363 *Aerosol Sci.*4: 411-419.

364 Fuchs, N. A. The Mechanics of aerosols. Macmillan Company, New York, 1964.

365 Goldberg, L.J. (1971). Naval Biomedical Research Laboratory, Programmed Environment,  
366 Aerosol Facility. *Appl. Microbiol.* 21: 244-252.

367 Goldberg, I.J., Watkins, H.M.S., Boerke, E.E. and Chatigny, M. A. (1958). The Use of a Rotating  
368 Drum for the Study of Aerosols over Extended Periods of Time. *Am. J. Epidemiol.* 68 :  
369 85-93.

370 Gruel, R.L., Reid, C.R. and Allemann, R.T. (1987). The Optimum Rate of Drum Rotation for  
371 Aerosol Aging. *J. Aerosol Sci.* 18: 17-22.

372 Haddrell, A.E. and Thomas, R.J. (2017). Aerobiology: Experimental Considerations,  
373 Observations, and Future Tools. *Appl. Environ. Microbiol.* 83: e00809-00817.

374 Ho, K.T. (2006). Evaluation of Test Method of Indoor Air Cleaners. Master thesis . Institute of  
375 Occupational Medicine and Industrial Hygiene, College of Public Health, National  
376 Taiwan University.

377 Huang, H.L., Lee, M.G. and Tai, J.H. (2012). Controlling Indoor Bioaerosols Using a Hybrid  
378 System of Ozone and Catalysts. *Aerosol Air Qual. Res.*12: 73-82.

379 Johnson, G.R., Knibbs, L.D., Kidd, T.J., Wainwright, C.E., Wood, M.E., Ramsay, K.A., Bell, S.C.  
380 and Morawska, L. (2016). A Novel Method and Its Application to Measuring Pathogen  
381 Decay in Bioaerosols from Patients with Respiratory Disease. *PLOS ONE* 11: e0158763.

382 Krumins, V., Son, E. K., Mainelis, G. and Fennell, D.E. (2008). Retention of Inactivated  
383 Bioaerosols and Ethene in a Rotating Bioreactor Constructed for Bioaerosol Activity



384 Studies. *CLEAN – Soil, Air, Water* 36: 593-600.

385 Kuo, Y. M. (2015) Field Evaluation of Sampling Bias with Plastic Petri Dishes for  
386 Size-Fractionated Bioaerosol Sampling. *Aerosol Sci. Tech.* 49:127-133.

387 Pich, J. (1972). Theory of Gravitational Deposition of Particles from Laminar Flows in Channels.  
388 *J. Aerosol Sci.*3: 351-361.

389 Piercy, T.J., Smither, S.J., Steward, J.A., Eastaugh, L. and Lever, M.S. (2010). The Survival of  
390 Filoviruses in Liquids, on Solid Substrates and in a Dynamic Aerosol. *J. Appl. Microbiol.*  
391 109: 1531-1539.

392 Ratnesar-Shumate, S., Pan, Y. L., Hill, S.C., Kinahan, S., Corson, E., Eshbaugh, J. and Santarpia,  
393 J.L. (2015). Fluorescence Spectra and Biological Activity of Aerosolized Bacillus Spores  
394 and Ms2 Bacteriophage Exposed to Ozone at Different Relative Humidities in a Rotating  
395 Drum. *J. Quant. Spectrosc. Radiat. Transf.* 153: 13-28.

396 Santarpia, J., L. , Sanchez, A.L., Lucero, G., Servantes, B. and Hubbard, J. (2014). A Laboratory  
397 Exposure System to Study the Effects of Aging on Super-Micron, Sandia national  
398 laboratories.

399 Santarpia, J.L., Pan, Y. L., Hill, S.C., Baker, N., Cottrell, B., McKee, L., Ratnesar-Shumate, S.  
400 and Pinnick, R.G. (2012). Changes in Fluorescence Spectra of Bioaerosols Exposed to  
401 Ozone in a Laboratory Reaction Chamber to Simulate Atmospheric Aging. *Opt. Express*  
402 20: 29867-29881.

403 Sutton, T. (2005). Decay of Particle Concentration as a Function of Rotation Rate in a Rotating  
404 Drum Chamber, U. S. Army research, development and engineering command.

405 TSI Inc. (2012). Model 3321 aerodynamic particle sizer spectrometer operation and service  
406 manual, P/N 1930092, Revision G. St. Paul, MN: TSI, Inc.

407 Turgeon, N., Michel, K., Ha, T. L., Robine, E., Moineau, S. and Duchaine, C. (2016). Resistance

408 of Aerosolized Bacterial Viruses to Four Germicidal Products. *PLOS ONE* 11: e0168815.

409 Verreault, D., Duchaine, C., Marcoux-Voiselle, M., Turgeon, N. and Roy, C.J. (2014). Design of  
410 an Environmentally Controlled Rotating Chamber for Bioaerosol Aging Studies. *Inhal.*  
411 *Toxicol.* 26: 554-558.

412 Verreault, D., Killeen, S.Z., Redmann, R.K. and Roy, C.J. (2013). Susceptibility of Monkeypox  
413 Virus Aerosol Suspensions in a Rotating Chamber. *J. Virol. Methods* 187: 333-337.

414 Verreault, D., Moineau, S. and Duchaine, C. (2008). Methods for Sampling of Airborne Viruses.  
415 *Microbiol. Mol. Biol. Rev.* 72: 413-444.

416 Wingstedt, E. M. M., Pedersen, K. and Reif, B. A, P. (2009). A modelling study of the flow  
417 pattern in a rotating drum for aerosol aging. Norwegian Defense Research Establishment  
418 (FFI) report 2009/01079.

419

420

### Figure Captions

421 **Fig. 1.** Schematic diagram of the experimental system.

422 **Fig. 2.** Decay kinetics of ambient aerosols by continuous sampling under rotation rates of 0, 5  
423 and 20 rpm.

424 **Fig. 3.** Aerosol decay as a function of particle size for continuous and intermittent sampling for  
425 the duration of 1 hour at a rotation rate of 5 rpm.

426 **Fig. 4.** Aerosol decay as a function of time for particles of different sizes.

427 **Fig. 5.** Aerosol decay over time as a function of particle size at 5 rpm. Symbols represent  
428 experimental data and solid lines represent the suspended aerosol fraction calculated from the  
429 decay constant of a half-hour measurement period. Long-dash lines and dotted lines represent the  
430 results of Gruel et al. (1987) and Asgharian and Moss (1992), respectively.

431 **Fig. 6.** Ratios of the experimental data and numerical data predicted by Gruel et al. (1987) and  
432 Asgharian and Moss (1992) as a function of particle size at 5 rpm after 1, 4 and 24-hr suspension  
433 periods.

434 **Fig. 7.** Aerosol decay as a function of particle size. Symbols represent experimental data under  
435 different rotation conditions. Long-dash lines and dotted lines represent the results of Gruel et al  
436 (1987) and Asgharian and Moss (1992), respectively.

437 **Fig. 8.** Ratios of experimental data and numerical data respectively predicted by Gruel et al.  
438 (1987) and Asgharian and Moss (1992) as a function of particle size at 0, 5 and 20 rpm after 1-hr  
439 suspension period.

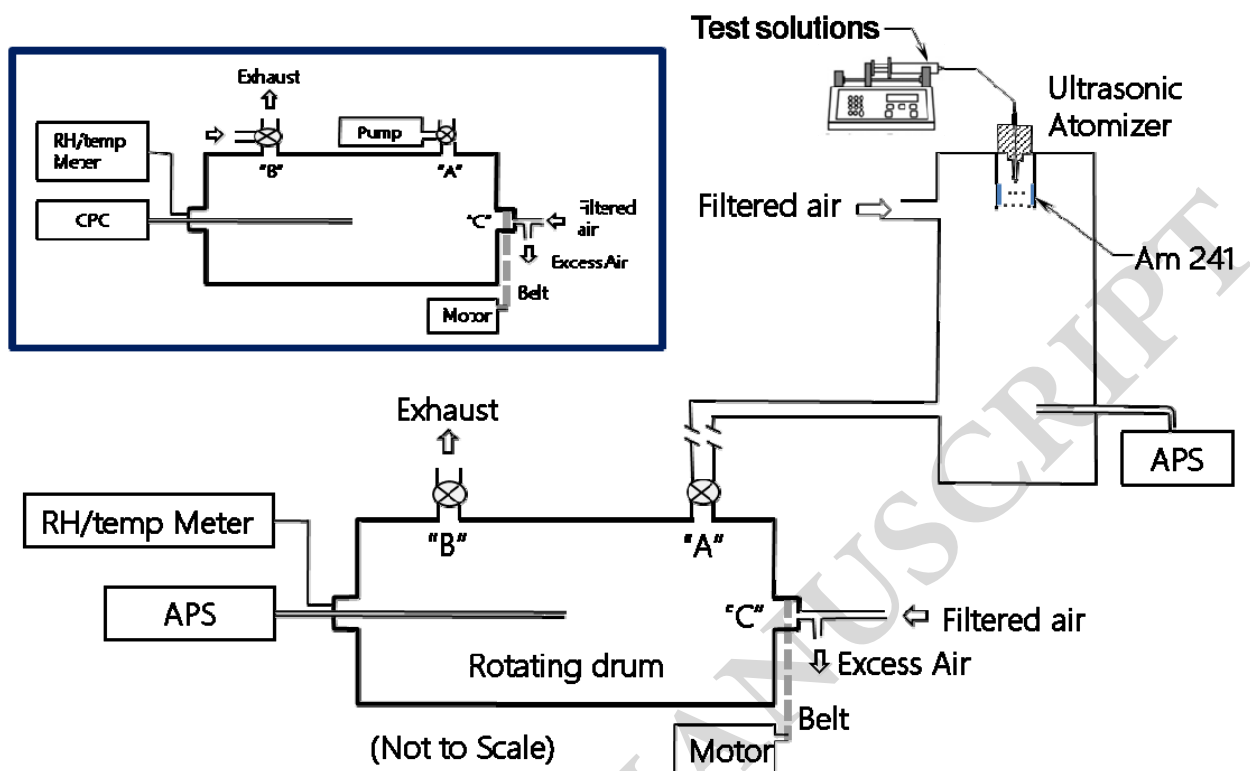
440 **Fig. 9.** Effect of rotation rate on aerosol decay constant as a function of particle size.

441 **Fig. 10.** Optimal rotation rates versus particle size.

442 **Fig. 11.** Aerosol retention time isopleths.

443

444

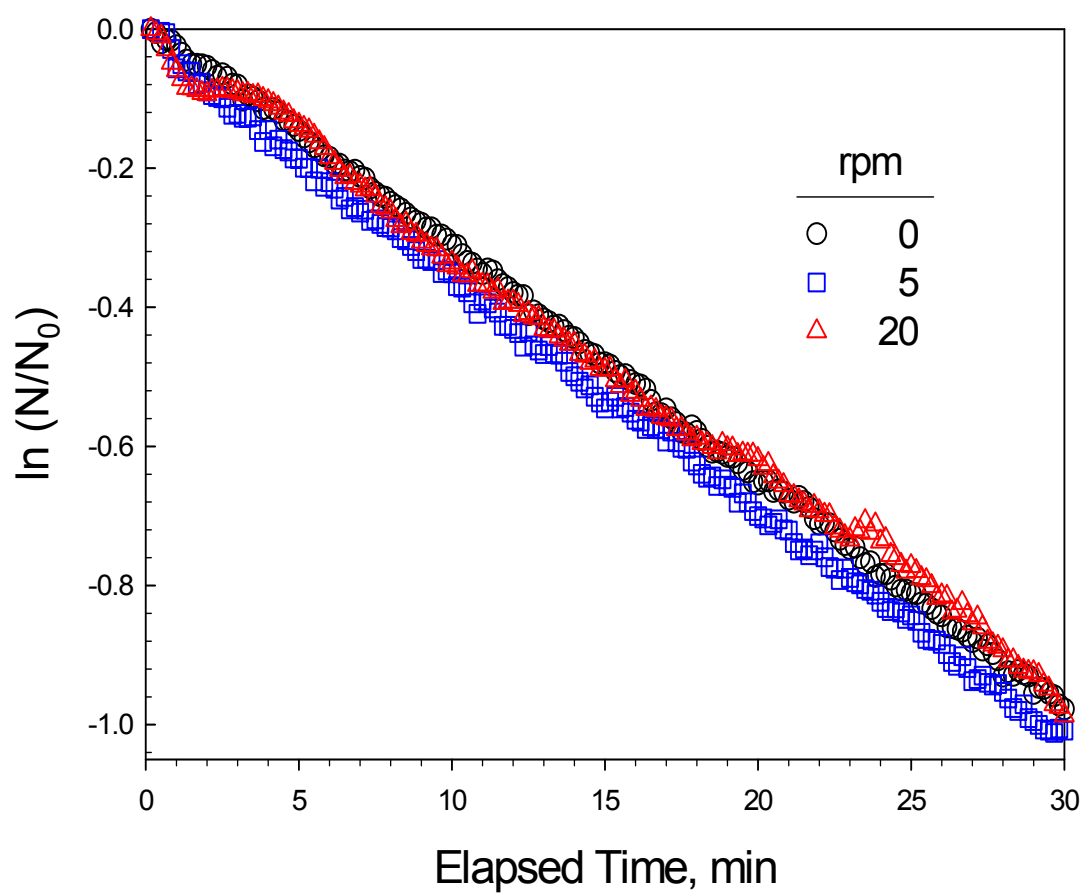


445

446

447

Fig. 1.



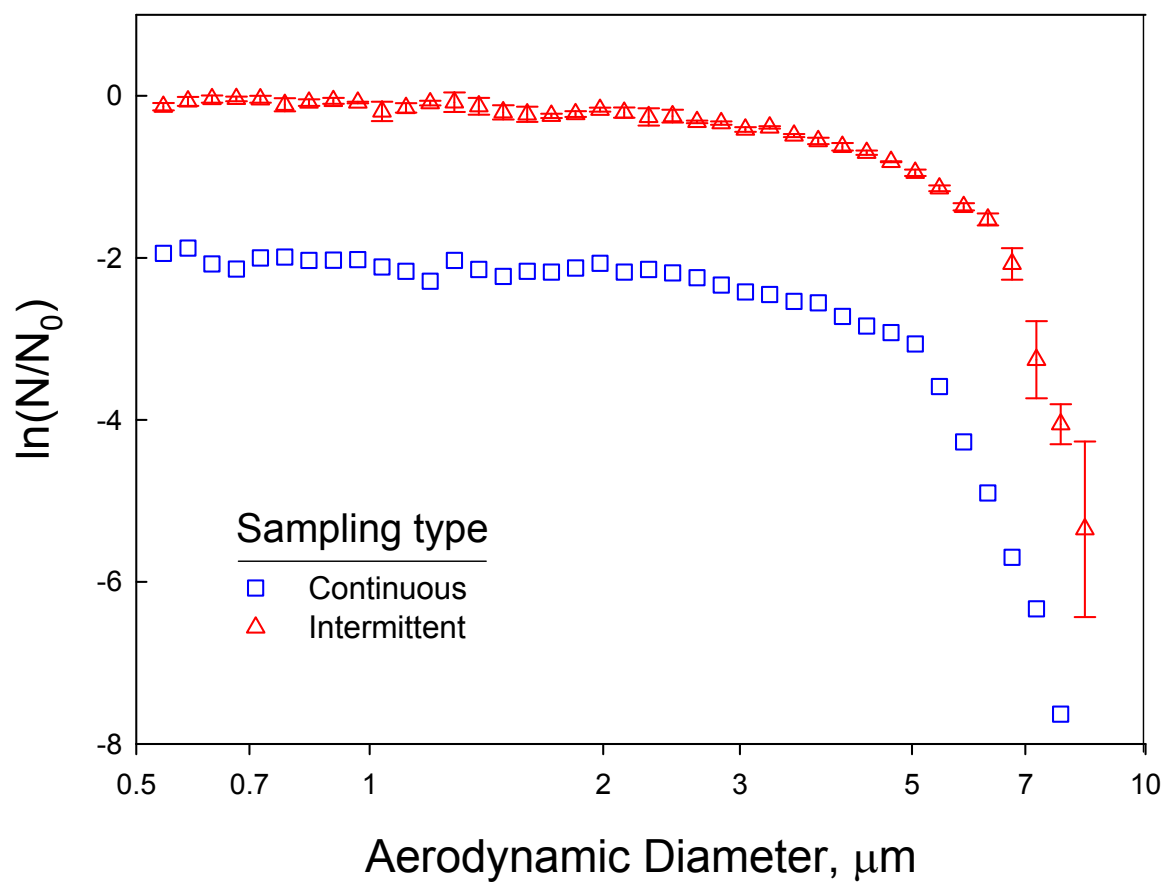
449

450

451

Fig. 2.

ACCEPTED



453

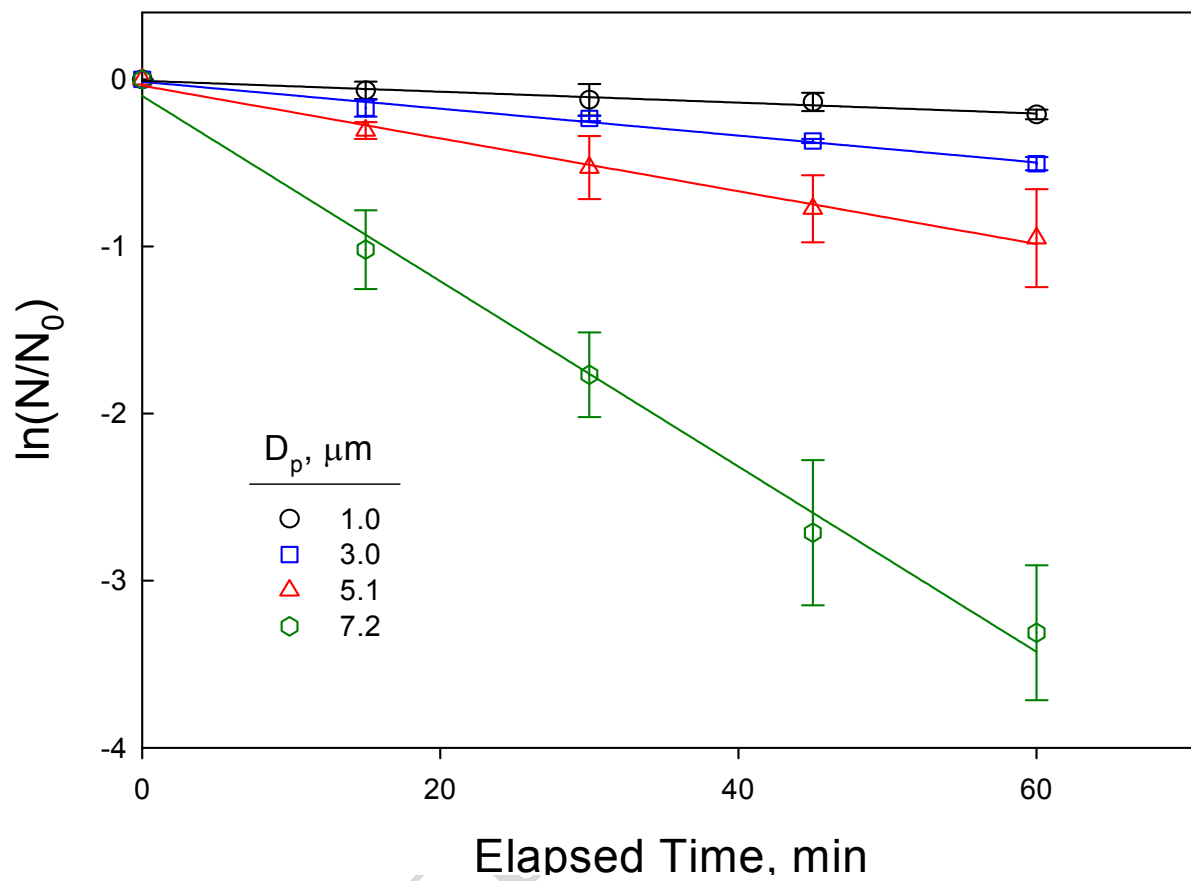
454

455

Fig. 3.

ACCEPTED

456



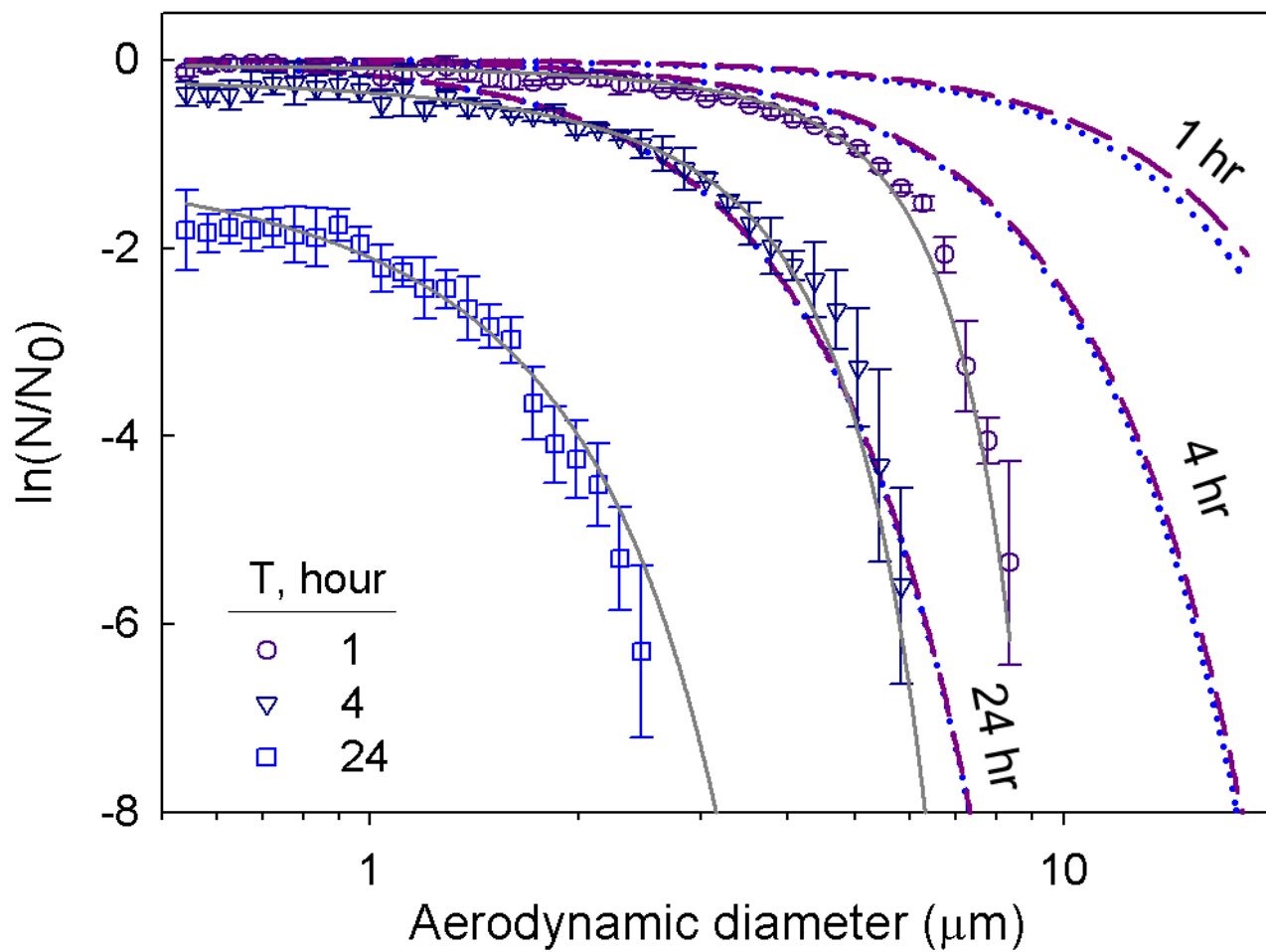
457

458

459

Fig. 4.

ACCEPTED



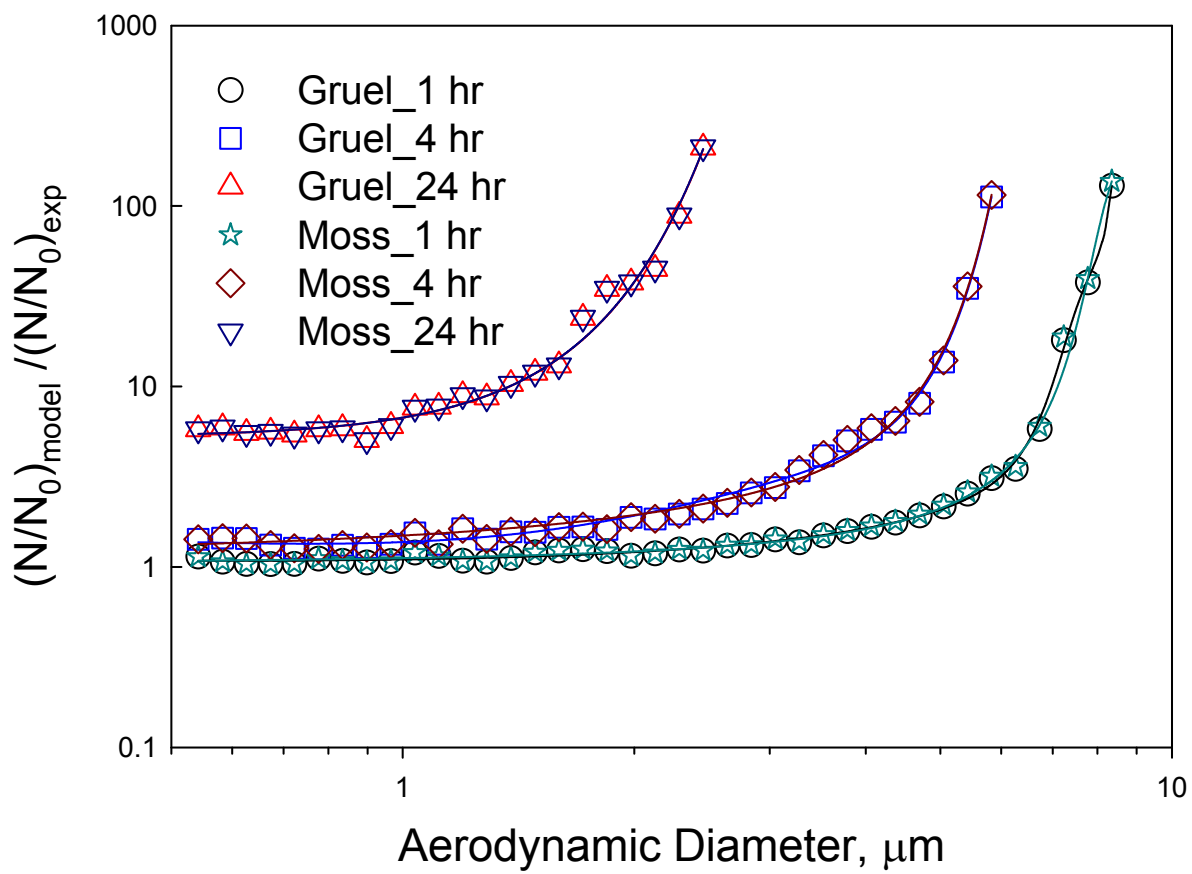
461

462

463

Fig. 5.





465

466

467

Fig. 6.

ACCEPTED

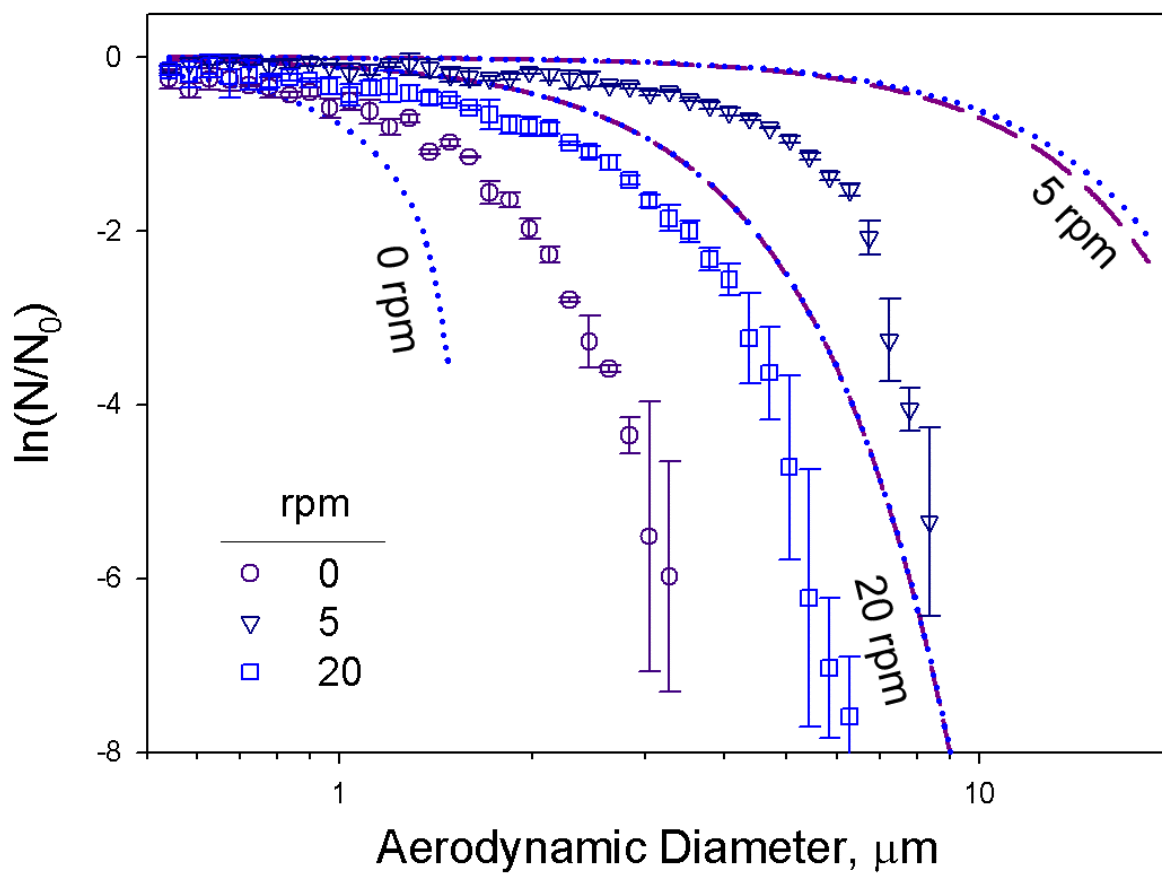
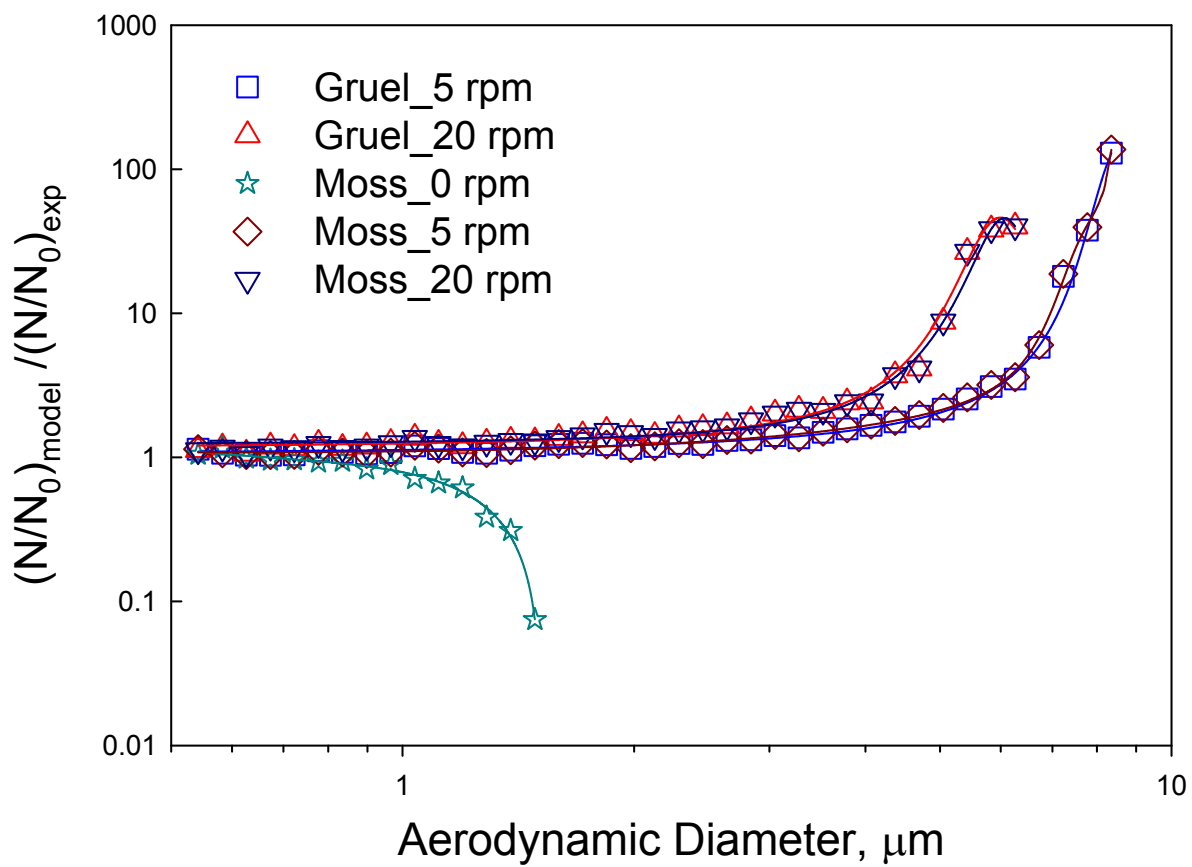


Fig. 7.



473

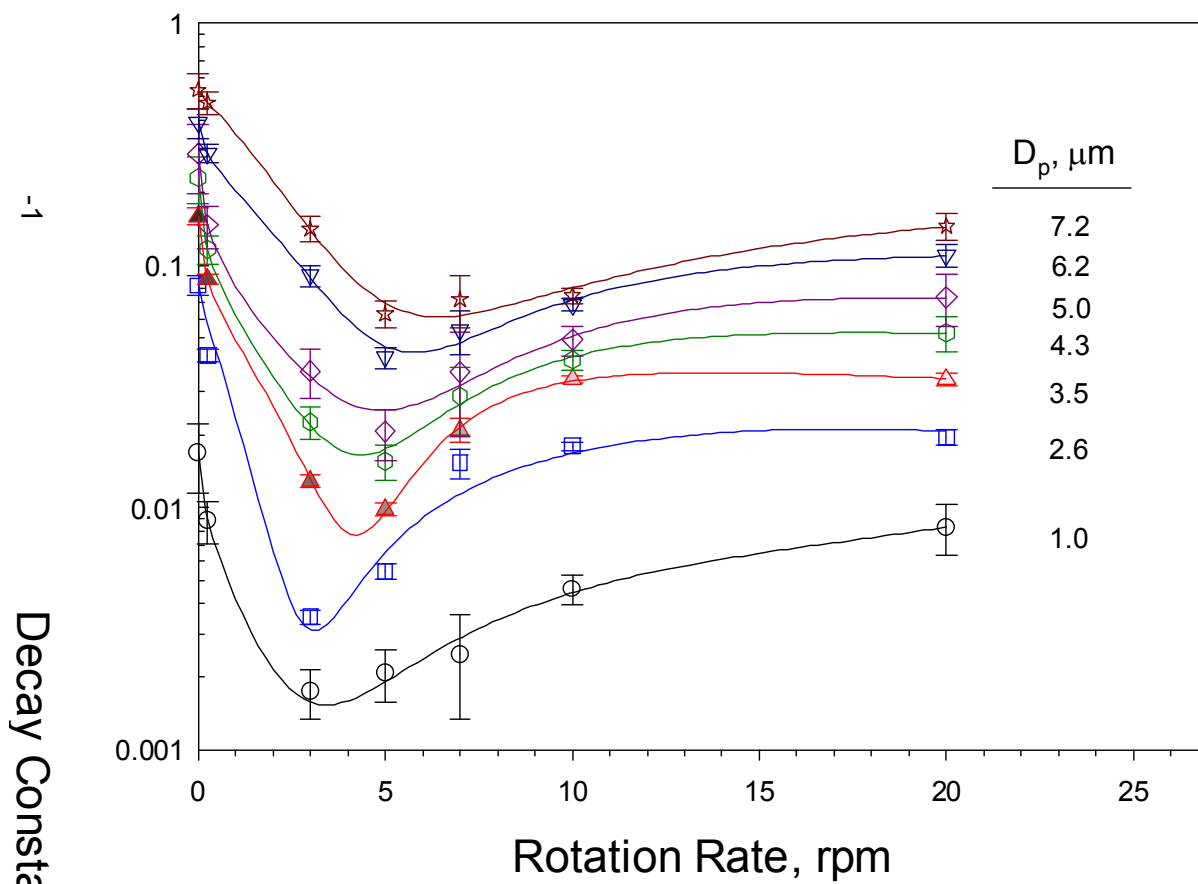
474

475

Fig. 8.

476

477



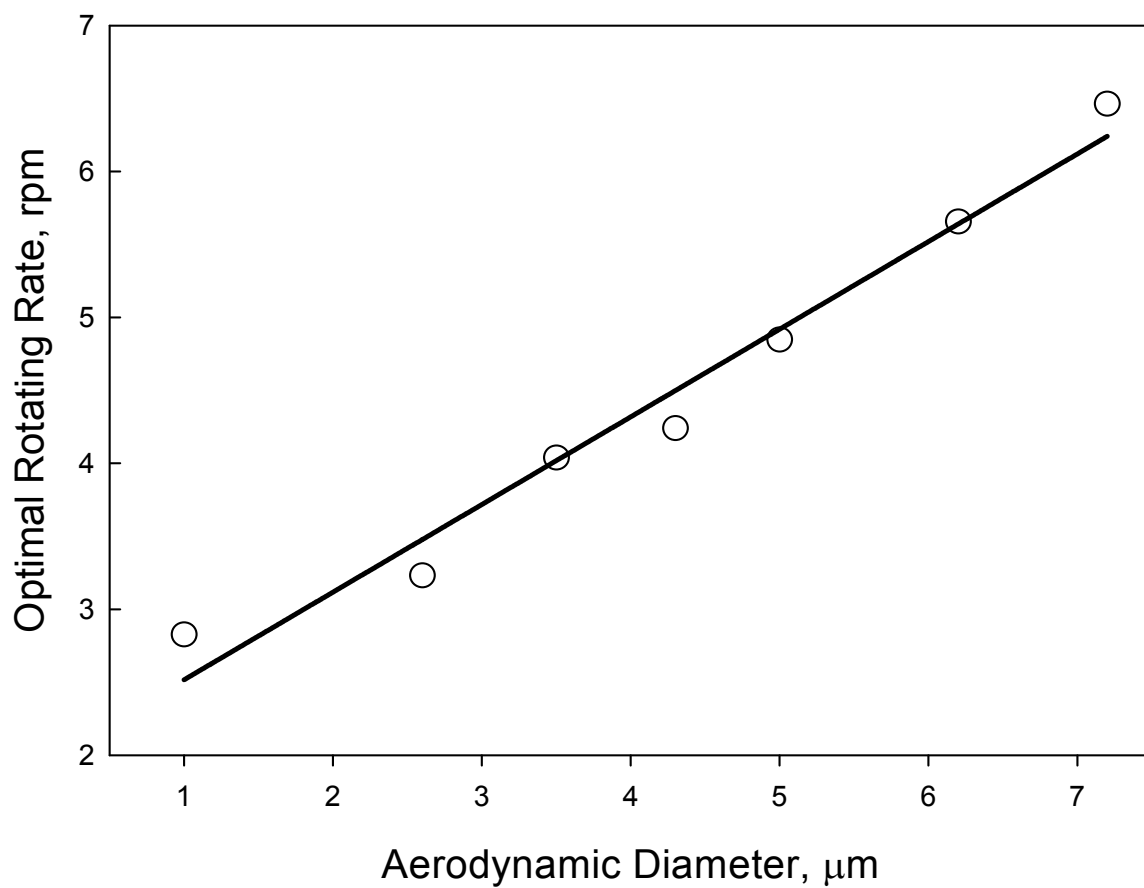
478

479

480

Fig. 9.

481



482

483

484

**Fig. 10.**

ACCEPTED

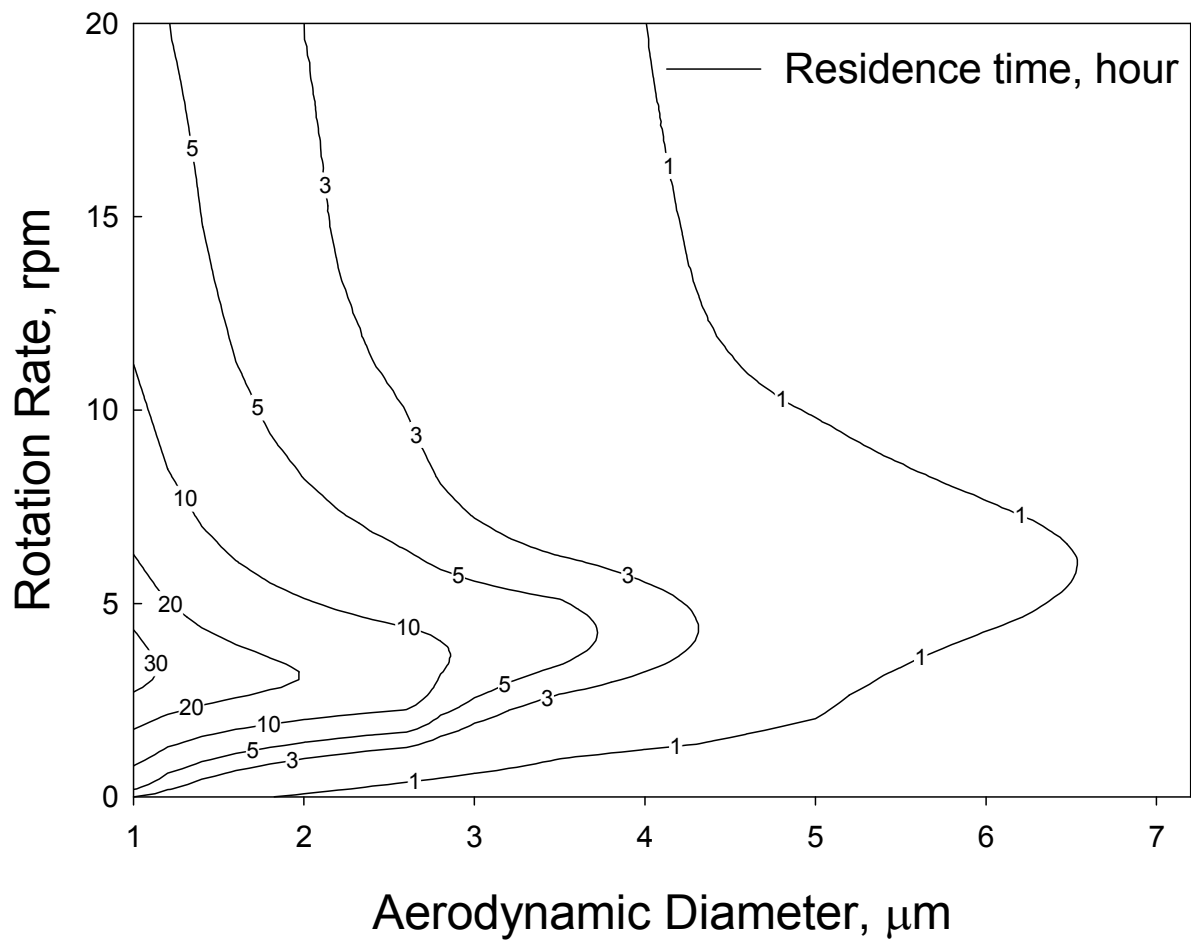


Fig. 11.